Journal of Materials Chemistry A

Accepted Manuscript

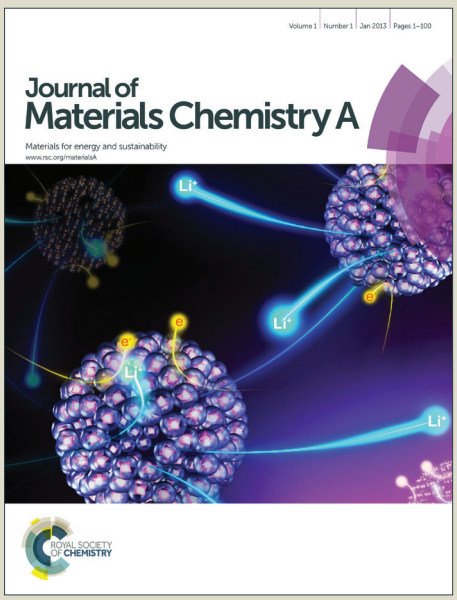

ROYAL SOCIETY OF CHEMISTRY

www.rsc.org/materialsA

Journal of Materials Chemistry A RSCPublishing

ARTICLE

A surfactant-modulated fluorescent sensor with pattern recognition capability: sensing and discriminating multiple heavy metal ions in aqueous solution

Cite this: DOI: 10.1039/xoxxoooooox

Received ooth January 2012,
Accepted ooth January 2012

DOI: 10.1039/xoxxoooooox

www.rsc.org/

Yuan Cao, Liping Ding*, Wenting Hu, Junxia Peng and Yu Fang

Pattern recognition has been widely used to detect and identify multiple analytes. Strategies of realizing pattern recognition of a single sensor are highly demanded. In the present work, a particular bispyrene-based fluorophore containing a hydrophilic spacer, Py-TOA-Py, was synthesized, and its mixture with anionic surfactant assemblies realizes multiple fluorescence responses to different metal ions. The combination of fluorescence variation at four emission wavelengths enables the fluorophore/surfactant sensor system to provide specific recognition patterns to different metal ions. Principle component analysis shows that the present single sensor system could discriminate 6 metal ions including Fe^{3+}, Co^{2+}, Ni^{2+}, Cu^{2+}, Pb^{2+}, and Hg^{2+}, 5 of which are heavy metal ions. Results from UV-vis measurements rule out the possibility of the bispyrene fluorophore binding with metal ions. Fluorescence titration of metal ions to two other bispyrene fluorophores finds that the one with similar hydrophilic spacer, Py-EOA-Py, exhibits similar multiple fluorescence responses, whereas, the one with hydrophobic spacer, Py-DDA-Py, displays none cross-reactive responses. Time-resolved emission spectra measurements reveal that the spacer polarity plays an important role in determining the location of bispyrene in surfactant assemblies, which further influences its cross-reactive responses to metal ions. The present work provides a new strategy of developing fluorescent sensors with pattern recognition abilities.

Introduction

Fluorescent molecular sensors have drawn continuous attention in fundamental research work and practical applications due to they possess high sensitivity and selectivity in detecting analytes.[1, 2] A typical fluorescent molecular sensor is usually consisted of a fluorophore for signal output, a receptor for binding analytes, and a spacer for chemically linking these two functional units.[1] For detecting various target analytes, different selective receptor units are usually needed to be specially designed and chemically derived on a selected fluorophore via an organic spacer. Although numerous fluorescent sensors with high sensitivity and selectivity have been developed, it is still a big challenge to meet the requirements to detect the vast variety of analytes of interest in the field of environmental protection, food and medicine safety, and medical diagnosis.

Inspired by the nature of the sensing of smell and taste, researchers devote into developing fluorescent sensor arrays containing a series of sensor elements to provide recognition patterns to different analytes.[3, 4] Such an array demands fewer requirements for selectivity of the receptor of each sensor element, and depends more on the cross-reactive properties of the used sensor elements. People usually choose different fluorophores or different receptors to generate an array of sensors and to provide cross-reactive responses to analytes,[5, 6] where combining the differential responses from each of these sensor elements to a typical analyte can generate a specific recognition pattern to the analyte. Thus, such a sensor array possesses high throughput in sensing and identifying different analytes. However, although such a method reduces dependence on synthetic efforts, better discriminative properties of an array depend on using large numbers of sensor elements. This, to some extent, restricts the applicability of pattern recognition. A suitable but simple and powerful technique to tune the sensory capability without need of heavy synthetic efforts is attractive in developing fluorescent sensors with pattern recognition ability.[7]

Surfactants are well-known amphiphilic molecules and can form various supramolecular assemblies such as micelles and vesicles in aqueous solutions.[8, 9] These assemblies are heterogeneous and possess a hydrophobic core and a hydrophilic surface. Such microheterogeneous structures enable surfactant aggregates to encapsulate lipophilic fluorophores and to construct fluorescent sensors with high sensitivity and selectivity.[10, 11] A number of advantages have been reported in using surfactant aggregates for developing fluorescent sensors. For instance, the sensitivity of a

fluorescent molecular sensor can not only be enhanced by using surfactant assemblies, but also be easily tuned by simply adjusting the co-existing surfactant concentration.[12-14] Moreover, surfactant assemblies with surface charges can function as noncovalent receptors to counterions. For example, aggregates of anionic surfactant such as sodium dodecyl sulfate (SDS) have been used in fabricating fluorescent sensors to metal ions such as Cu^{2+} and Hg^{2+}.[15, 16] On the contrary, assemblies of cationic surfactants like dodecyl trimethyl ammonium bromide (DTAB) have been used in developing fluorescent sensors to anionic ions such as S^{2-}, F^-, and CN^-.[12, 17-19]

Additionally, the container properties of surfactant assemblies have been recently used in developing fluorescent sensor arrays with pattern recognition ability. Anslyn and co-workers reported using Tween 80 micelles as containers to dissolve four different types or concentrated fluorophores and fabricate a sensor array providing seven-signal pattern to a typical explosive analyte.[20] Thayumanavan and co-workers developed a strategy of using complexes of surfactant and polyelectrolyte to form supramolecular assemblies for encapsulating different fluorophores to provide pattern recognitions to proteins.[7] The addition of proteins could disassemble the complexes and release those encapsulated fluorophores, which results in various fluorescence changes of different fluorophores. Moreover, by simple varying the structure and charge of surfactant and polyelectrolyte, they realized the pattern recognition of proteins using a single fluorescent guest.[21] The noncovalent interaction between fluorophore and surfactant assemblies provides a simple but powerful way to tune the sensory performances.

It is known that many of heavy metal ions are highly toxic and involved in serious diseases. Therefore, intense attention has been paid to developing fluorescent sensors and arrays for detection of multivalent transition metal ions (especially heavy metal ions) due to the increasing concerns on environmental protection and human health.[6, 22-24] However, most of the reported fluorescent sensor arrays for metal ions have focused on using different fluorophores to derive and synthesize multiple sensor elements. As mentioned earlier, such strategy requires tedious synthesis effort and complex data collecting process. It is in great demand and a big challenge to develop fluorescent sensors capable of pattern recognition of multiple metal ions in aqueous solutions.

In the present work, we aim to construct a fluorescent sensor platform for pattern recognition of multiple metal ions by using the noncovalent modulation ability of surfactant assemblies. Considering the targets are cationic metal ions, the anionic surfactant SDS will be used to provide negative aggregation surface for attracting metal ions as well as heterogeneous containers for fluorophores. A bispyrene fluorophore containing a hydrophilic oligo(oxyethylene) unit in spacer was specially designed and synthesized (Scheme 1). Pyrene was selected as the reporter unit not only because it has high quantum yield and long lifetime, and is easy to be derived, but also because it emits multiple fluorescence signals in forms of structured monomer emission at shorter wavelengths and broad structureless excimer emission at longer wavelengths. Thus, the noncovalent binding of metal ions to SDS aggregates may induce multiple fluorescence variations of the bispyrene fluorophore and result in multiple fluorescence response signals at different wavelengths. Fluorescence titration of different metal ions reveals that the fluorophore-surfactant assemblies could function as a pattern recognition sensor to several heavy metal ions.

Experimental

Chemicals and instruments

4,7,10-Trioxa-1,13-tridecanediamine (TOA, 98%), 1,2-bis(2-aminoethoxy)-ethane (EOA, 98%), 1,12-diaminododecane (DDA, 98%), and sodium dodecyl sulfate (SDS, 98%) were all purchased from Sigma-Aldrich company and used without further purification. Pyrene (Alfa, 98%) was used after recrystallization by ethyl alcohol. Pyrenesulfonyl chloride (PSC) was synthesized by adopting a literature method.[25] $Fe(NO_3)_3\ 9H_2O$, $Cu(NO_3)_2\ 3H_2O$, $Co(NO_3)_2\ 6H_2O$, $Zn(NO_3)_2\ 6H_2O$, $Mg(NO_3)_2\ 6H_2O$, $Pb(NO_3)_2$, $Ca(NO_3)_2\ 4H_2O$, $Ni(NO_3)_2\ 6H_2O$, $Cd(NO_3)_2\ 4H_2O$, and $HgCl_2$ are analytically pure and dissolved in water to obtain 2.5×10^{-3} M stock solutions. SDS was dissolved in water to prepare aqueous solution with required concentrations. Analytical pure acetonitrile and trichloromethane were dried with anhydrous $CaCl_2$ overnight before use. Aqueous solutions were prepared from Milli-Q water (18.2 MΩ cm at 25 ℃). All other reagents are at least analytical pure.

^1H NMR and ^{13}C NMR spectra were measured on Bruker AV 400 MHz NMR spectrometer. The high resolution mass spectra (MS) were acquired in ESI positive mode using Bruker maxis UHR-TOF Mass Spectrometer. The FTIR spectra were measured on a Fourier Transform Infrared Spectrometer (Vertex 70v, Bruker, Germany). Fluorescence measurements were conducted at room temperature on a time-correlated single photon counting fluorescence spectrometer (Edinburgh Instruments FLS 920). For steady-state fluorescence measurements, all samples were excited at 350 nm using xenon light as excitation source. For time-resolved measurements, all solutions were excited at 343 nm using laser (343.4 nm) as excitation source, and the emission wavelength was set to 500 nm for pyrene decays. UV-vis absorption spectra were recorded on a spectrophotometer (Lambda 950, Perkin-Elmer, USA).

Synthesis of N,N'-(((oxybis(ethane-2,1-diyl))bis(oxy)) bis(propane-3,1-diyl))bis(pyrene-1-sulfonamide) (Py-TOA-Py)

The bispyrene derivative containing oligo(oxyethylene) as a linker, Py-TOA-Py, was synthesized by reacting pyrenesulfonyl chloride (PSC) with the α,ω-diamine compound, 3,3'-((oxybis(ethane-2,1-diyl))-bis(oxy))-bis(propan-1-amine) (TOA). The synthesis procedure is as follows: 0.1 mL of TOA (0.45 mmol) was added into a solution of PSC (302 mg, 1.0 mmol) in $CHCl_3$ (200 mL) under stirring and N_2 atmosphere, then refluxed over a period of 24 h. After the mixture was cooled to room temperature, it was washed with brine until the pH of the aqueous layer is neutral. Organic layers were combined and dried with anhydrous Na_2SO_4 overnight and filtered. The filtrate was evaporated under reduced pressure. Resulting yellow-green oil was purified by column chromatography on silica gel column with CH_2Cl_2:CH_3OH (*v*:*v*, 50:1) as eluent. Py-TOA-Py was obtained as a yellow solid after freeze-drying (273 mg, yield 82%). The synthesis route of Py-TOA-Py is shown in scheme 1. ^1H NMR (400 MHz, $CDCl_3$, ppm): δ 8.95 (d, J = 9.4 Hz, 1H), 8.66 (d, J = 8.2 Hz, 1H), 8.22 – 8.01 (m, 7H), 6.03 (t, J = 5.4 Hz, 1H), 3.63 (dd, J = 5.5, 3.4 Hz, 2H), 3.51 (dd, J = 5.5, 3.4 Hz, 2H), 3.36 (t, J = 5.5 Hz, 2H), 3.07 (dd, J = 11.5, 5.7 Hz, 2H), 1.58 – 1.52 (m, 2H). ^{13}C NMR (101 MHz, $CDCl_3$, ppm): δ 134.72, 131.82, 131.03, 130.28, 130.07, 129.94, 128.14, 127.51, 127.14, 126.87, 126.78, 125.28, 124.15, 123.90, 123.58, 77.48, 76.84, 70.72, 70.22, 42.43, 28.69. FTIR (KBr plate, cm^{-1}): 3283 (–NH), 3044 (Ar–H), 2922 (–CH_2), 1588 (Ar C=C), 1325 (–C–N), 1158 (O=S=O), 1093 (–C–O–C). MS (ESI) $[M+Na]^+$: calcd. for $C_{42}H_{40}N_2O_7S_2Na$, 771.2175; found, 771.2173.

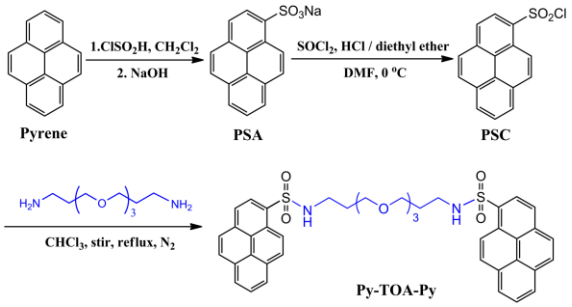

Scheme 1. Synthesis route of Py-TOA-Py.

Results and discussion

UV-vis absorption and fluorescence emission of Py-TOA-Py in neat solvents

The absorption and emission spectra of Py-TOA-Py were first examined in its good solvent (acetonitrile) and poor solvent (water), and the result is illustrated in Fig. 1. In acetonitrile, Py-TOA-Py shows strong absorptions at 279 and 351 nm (ε_{351} = 2.4 × 10^5 L·mol^{-1}·cm^{-1}). In neat water, the absorption spectra red-shift with the maximum emission at 283 and 355 nm. The molar coefficient at 355 nm in water was determined to be 6.5 × 10^4 L·mol^{-1}·cm^{-1}, which is ca. 27% of that in acetonitrile.

As to the emission spectra, Py-TOA-Py (1.0 μM) exhibits strong excimer emission in both solvents but shows quite different monomer emission. In acetonitrile, the fluorophore displays apparent monomer emission at 380 and 400 nm, whereas, in water, the monomer emission is extremely weak compared to excimer emission. These results suggest that the fluorphore is well dispersed in the good solvent, acetonitrile, whereas, in the poor solvent, water, the hydrophobic pyrene moieties tend to aggressively aggregate.

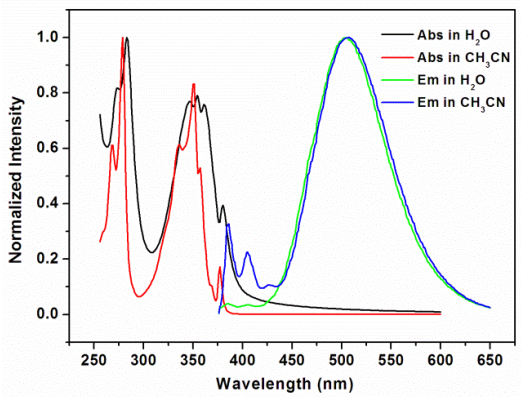

Fig. 1 UV-vis absorption and fluorescence emission spectra of Py-TOA-Py in acetonitrile and water.

The strong aggregation in water leads to unstable fluorescence emission. Over a period of 60 minutes, the fluorescence emission appears very stable in acetonitrile, but decreases and fluctuates in water (c.f. Fig. S1 in the Supporting Information (SI)), which makes the fluorophore unsuitable to function as sensor in water. Fortunately, the introduction of anionic surfactant SDS could significantly enhance the fluorescence stability of Py-TOA-Py in aqueous solution, where the SDS concentration needs to be above 4 mM. As seen in Fig. S1, over a period of 60 min, the fluorescence intensity is barely changed in SDS aqueous solution as observed in the good solvent. This could be due to the dispersion of Py-TOA-Py into the hydrophobic microenvironments provided by the supramolecular assemblies of SDS in water. Thus, the Py-TOA-Py/SDS system could function as aqueous sensors for metal ions, which is more significant considering the increasing seriousness of water pollution.

SDS effect on fluorescence emission of Py-TOA-Py in water

We particularly investigate the concentration effect of surfactant on the emission spectra of Py-TOA-Py to evaluate the modulation behaviour of surfactant aggregates. The fluorescence spectra of the bispyrene fluorophore in different concentrated SDS aqueous solutions are displayed in Fig. 2. Clearly, the surfactant concentration has a distinct effect both on intensity and profile of the fluorescence emission of Py-TOA-Py. The gradual increasing SDS concentration from 4 mM to 12 mM leads to three stages of fluorescence variation: first, the fluorescence intensity of the fluorophore gradually enhances when SDS concentration increases from 4 mM to 7 mM, then, shows a distinct enhancement when SDS concentration reaches its CMC, 8 mM, and finally, reaches a plateau when SDS concentration is above its CMC (e.g., at 10 and 12 mM). This enhancement in fluorescence intensity could be due to the hydrophobic environment provided by SDS aggregates that reduce solvent effect and prevent oxygen quenching. As illustrated from the inset of Fig. 2, the ratio of monomer to excimer is also dependent upon SDS concentration, which indicates different assemblies of SDS adjust the relative distance between the two pyrene moieties and vary the ratio of excimer to monomer. Clearly, the formation of micelles facilitates monomer emission, which could be due to the encapsulation in SDS micelles that breaks the strong aggregation among bispyrene fluorophores.

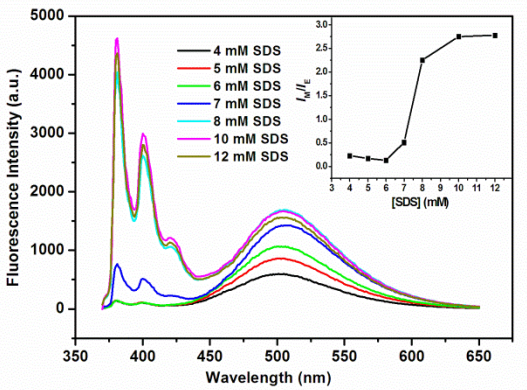

Fig. 2 Fluorescence emission of Py-TOA-Py in different concentrated SDS aqueous solutions (λex = 350 nm). Inset: Fluorescence intensity ratio of monomer to excimer of Py-TOA-Py as a function of SDS concentration.

Sensing behaviour to metal ions in SDS solutions

Considering the dramatically enhanced fluorescence stability and intensity in SDS solution, the following sensing studies were measured in SDS solutions. The SDS concentration was controlled at 7 mM since the fluorophore shows higher responses to the tested metal ions at this SDS concentration (Fig. S2 in the SI). The reason for this could be due to the competition of two processes: electrostatic interaction between SDS aggregates and metal ions and encapsulation of bispyrene fluorophore by SDS aggregates. The former process attracts more metal ions to the aggregate surface when increasing SDS concentration, which leads to higher sensitivity. However, the

latter case causes more bispyrene fluorophore to be encapsulated by SDS aggregates when increasing SDS concentration, which reduces the accessibility of fluorophores to metal ions and results in lower sensitivity. This phenomenon of surfactant concentration to modulate sensor's sensitivity has been found by others[14] and in our previous work[26].

Thus, the sensing behaviour of the sensor platform containing 1.0 μM of bispyrene fluorophore and 7 mM of SDS to 10 metal ions was thoroughly examined. The aqueous stock solutions of metal ions in nitrate or chlorate salts were gradually titrated into the detection system. Very interestingly, the sensor system exhibits two main different response modes to the 10 tested metal ions including Mg^{2+}, Ca^{2+}, Fe^{3+}, Co^{2+}, Ni^{2+}, Cu^{2+}, Zn^{2+}, Cd^{2+}, Pb^{2+}, and Hg^{2+} ions. The first mode is turn-off response, where the fluorescence emission is gradually quenched along increasing metal ion concentration. This is observed for Fe^{3+}, Cu^{2+}, and Hg^{2+}, which are shown in Fig. 3a, 3b, and S3 (SI), respectively. However, a close examination of these figures could find that the quenching extent of the sensor system is various to different metal ions. For example, the excimer emission is significantly quenched by both Fe^{3+} and Cu^{2+}, whereas, the excimer quenching extent by Hg^{2+} is much smaller. Particularly, the addition of 70 μM of Fe^{3+} leads to 85~90% reduction of excimer emission, and the addition of 30 μM of Cu^{2+} produces 87~88% decreasing of excimer emission. By comparison, the addition of 20 μM of Hg^{2+} reaches the highest extent of excimer quenching, and causes only 40~42% of excimer quenching. Besides excimer, the monomer quenching extent is also different for these metal ions. The monomer emission can be effectively quenched by gradual addition of Fe^{3+}. By contrast, this monomer quenching effect is much less apparent upon gradual addition of Cu^{2+}. Low concentration of Hg^{2+} (below 20 μM) could also produce effective monomer quenching, but further increasing Hg^{2+} concentration leads to no apparent additional quenching.

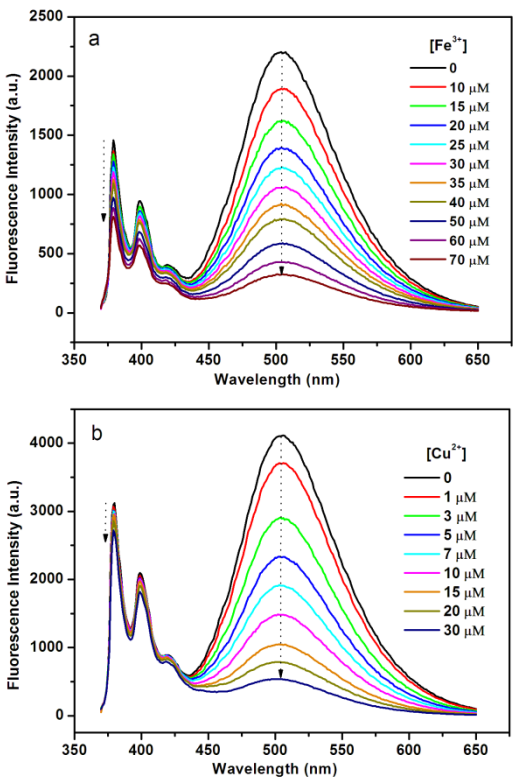

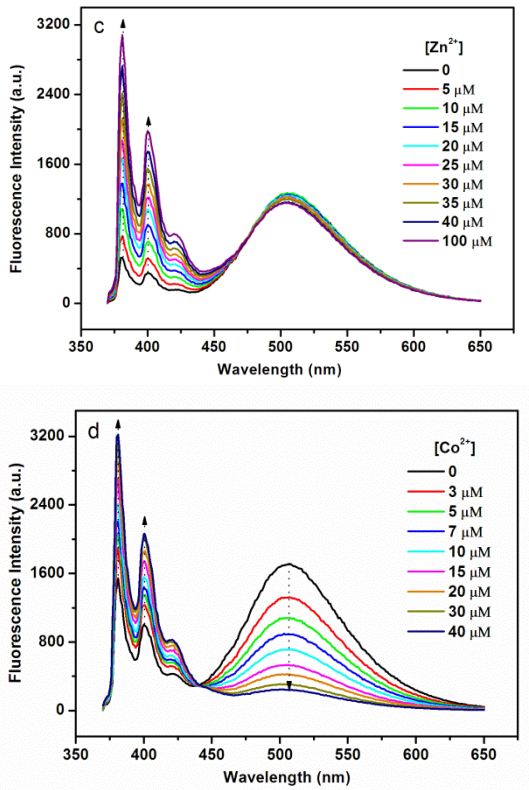

Fig. 3 Fluorescence spectra of Py-TOA-Py (1.0 μM) in 7 mM SDS aqueous solution upon addition of different metal ions: (a) Fe^{3+} ion; (b) Cu^{2+} ion; (c) Zn^{2+} ion; (d) Co^{2+} ion. (λex = 350 nm).

The second mode is ratiometric response, where an enhanced monomer emission is accompanied with a decreased excimer emission via an isoemissive point. This phenomenon is observed for the titration of the rest 7 examined metal ions. However, a big difference exists in this ratiometric response to different metal ions. As shown in Fig. 3c and 3d, the monomer emission is remarkably enhanced upon proportional addition of both Zn^{2+} and Co^{2+}. However, the excimer emission is slightly decreased upon titration of Zn^{2+}, but significantly reduced upon titration of Co^{2+}. The former case is also discovered for Mg^{2+}, Ca^{2+}, and Cd^{2+} ions (Fig. S4 in the SI), and the latter case is also found for Ni^{2+} and Pb^{2+} (Fig. S5 in the SI) except that the quenching of excimer is largely varied from ion to ion.

The multiple fluorescence responses of the present sensor system to different metal ions can also be visualized by exposure to 365 nm UV light. The photos of the sensor solution in the presence of 50 μM of Fe^{3+}, Cu^{2+}, Zn^{2+}, and Co^{2+} under 365 nm UV light are illustrated in Fig. 4. It can be seen that the green emission of the sensor solution is significantly quenched by addition of Fe^{3+}, which agrees with the results of the notable reduction of both monomer and excimer emission induced by Fe^{3+}. A weak blue is observed for addition of Cu^{2+}, which originates from the left slightly quenched monomer emission. A stronger blue emission is revealed for addition of Co^{2+}. This is because in comparison with Cu^{2+}, the monomer emission is remarkably enhanced by Co^{2+}. As to addition of Zn^{2+}, a green-blue colour is observed, which is in agreement with the combination of the remarkable monomer emission and the left slightly-decreased excimer emission.

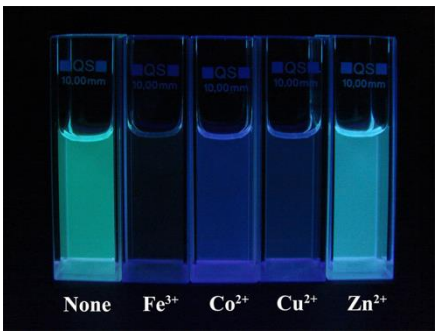

Fig. 4 Photos of solutions of Py-TOA-Py/SDS in the absence and presence of metal ions (50 μM) under illustration of 365 nm UV light.

This versatile fluorescence response of the present sensor to different metal ions may enable it to provide recognition patterns to these metal ions by combining the fluorescence responses at different wavelengths, which will then make it a discriminative sensor. Therefore, we collected the fluorescence variations at four selected wavelengths (382, 402, 460, and 500 nm) which can be interpreted as four traditional sensor elements used in sensor arrays. These four wavelengths are chosen because they represent two monomer emission peaks, distorted excimer emission position, and the perfect excimer emission center, respectively.[27] For expressing the changing pattern more unambiguous and visualized, the fluorescence variation was calculated by $\lg(I/I_0)$ and displayed in Fig. 5, where I_0 and I are the fluorescence intensity at the corresponding wavelength in the absence and presence of metal ions (10 μM). As can be seen from the bar chart that the array of the four wavelengths can generate a distinct pattern response (fingerprint) to some of the metal ions, suggesting the present sensor system could discriminate different metal ions.

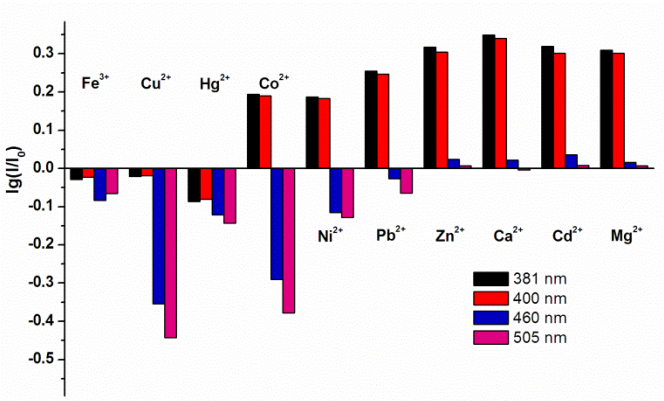

Fig. 5 Recognition patterns for metal ions (10 μM) by collecting fluorescence quenching data at four selected wavelengths.

Principal component analysis (PCA) has been widely utilized to analyse the pattern recognition ability of sensor arrays by reducing the dimensionality of the data set.[28, 29] Therefore, PCA was performed to evaluate the discriminatory power of the present sensor platform. For this purpose, the fluorescence variation of Py-TOA-Py/SDS at the four selected wavelengths to the tested metal ions at different concentrations was collected for PCA analysis. The resulting two-dimensional plots are shown in Fig. 6. As observed, the first principle component (PC1) carries ca. 80.6% of the variance while the second principle component (PC2) carries ca. 19.2%. Altogether these two components carry about 99.8% of the whole variance. It can be seen that the two dimensional score plot for the first two principal components (PC1 and PC2) can provide seven well separated clustering for Fe^{3+}, Cu^{2+}, Co^{2+}, Ni^{2+}, Pb^{2+}, Hg^{2+}, and for Zn^{2+}, Ca^{2+}, Cd^{2+} and Mg^{2+} together. However, the separation among Zn^{2+}, Ca^{2+}, Cd^{2+}, and Mg^{2+} is hard as they produce similar ratiometric response modes. Even though, the present sensor is capable of identifying at least 6 different metal ions including Fe^{3+}, Cu^{2+}, Co^{2+}, Ni^{2+}, Pb^{2+}, and Hg^{2+}. It is well known that Pb^{2+} and Hg^{2+} are highly toxic heavy metal ions and of serious environmental concern.[24] At the same time, Cu^{2+}, Co^{2+}, and Ni^{2+} are also concerned heavy metal pollutants and important factors involved in many diseases.[23, 26, 30] This makes the present sensor system a powerful tool in detecting multiple heavy metal ions. Moreover, discrimination of chemically similar analytes is usually accomplished by the utilization of sensor arrays comprising of a series of cross-reactive sensor elements.[3] Most researchers interested in this field pursue smallest number of sensor elements due to cumbersome synthesis and time-consuming data collecting and processing process.[22] So far, reports on the use of a single sensor to discriminate structurally similar compounds have been very rare,[21, 27, 31] which makes the present work more interesting and demands understanding the sensing mechanism of its multiple responses to different metal ions.

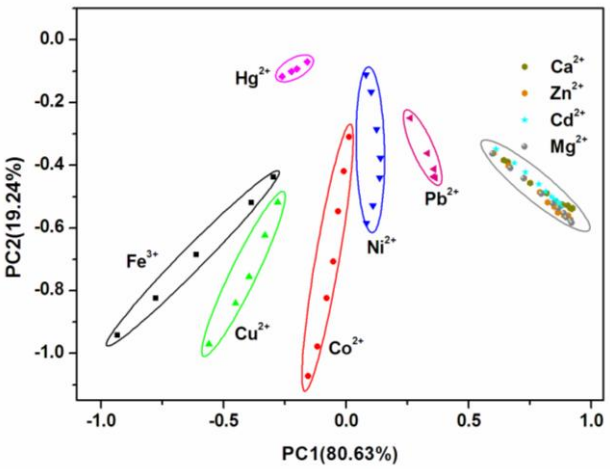

Fig. 6 Two-dimensional PCA score plot for discrimination of metal ions at different concentrations.

Sensing mechanism studies

The cross-reactive responses of the present sensor system to the 10 tested metal ions drive us to find out the reason of this phenomenon. Therefore, several experiments were conducted to explore the sensing mechanisms of the present supramolecular sensor system to metal ions. First of all, the UV-vis absorption of Py-TOA-Py in 7 mM SDS solution upon titration of different metal ions was measured to check the binding interaction of Py-TOA-Py with these metal ions. Fig. 7 displays the example result of the absorption spectra of Py-TOA-Py upon titration of Cu^{2+}, where the absorption spectra were characterized with typical pyrene absorption at 280 and 352 nm. It can be seen that the gradual addition of Cu^{2+} produces negligible variation in the absorption. This also occurs to the other metal ions such as Fe^{3+}, Zn^{2+}, and Co^{2+}. As illustrated in the inset of Fig. 7, the absorbance intensity variation A/A_0 of the fluorophore (monitored at 352 nm) is almost independent upon metal ion concentration in SDS aqueous solution, where A_0 and A are the absorbance intensity in the absence and presence of metal ions, respectively. It could be seen that the variation value of

absorption spectrum is less than 5% of origin intensity at all metal ion concentrations. Such results indicate that these metal ions do not form complexes with the bispyrene fluorophore, ruling out the possibility that the changes in fluorescence spectra are due to the direct binding metal ions with the fluorophore. Thus, it elicits that the multiple fluorescence variation upon different metal ions may be due to the versatile interaction between metal ions and SDS aggregates which further influence the fluorescence emission of Py-TOA-Py.

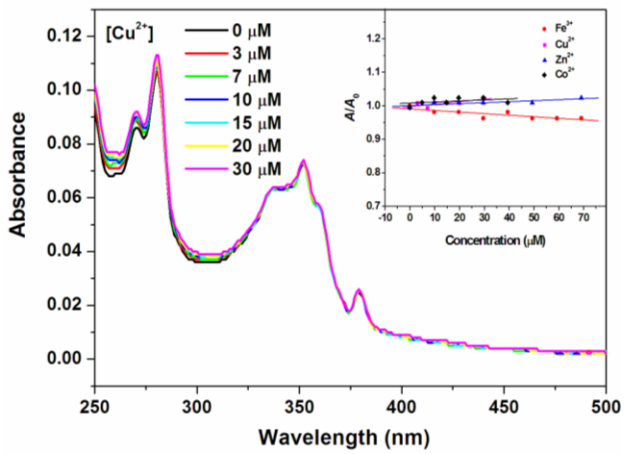

Fig. 7 Effect of addition of Cu^{2+} ions on the UV-vis spectra of Py-TOA-Py (1.0 μM) in 7 mM SDS aqueous solution. Inset: absorbance intensity variation of Py-TOA-Py (1.0 μM) to different concentrated metal ions in 7 mM SDS aqueous solution.

To further understand the sensing behaviour, we synthesized two other bispyrene compounds. One is an analogy compound N,N'-((ethane-1,2-diylbis(oxy))bis(ethane-2,1-diyl))bis(pyrene-1-sulfonamide) (Py-EOA-Py), the spacer of which contains two oxyethyl groups, one less than in the spacer of Py-TOA-Py. The other is a control compound, N, N'-(dodecane-1,12-diyl)bis(pyrene-1-sulfonamide) (Py-DDA-Py), the spacer of which has the same length as that of Py-TOA-Py but contains 12 methylene units with no oxyethyl groups. The structures of Py-EOA-Py and Py-DDA-Py are illustrated in Scheme 2. The synthesis routes of these two fluorophores are shown in Schemes S1 and S2 in the SI, and the detailed synthesis processes are also provided in the SI.

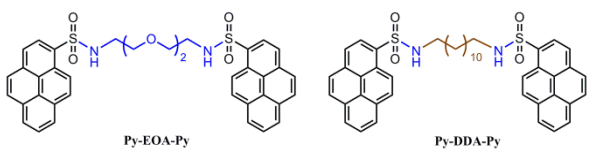

Scheme 2. Chemical structure of the analogy bispyrene fluorophore, Py-EOA-Py, and that of the control bispyrene fluorophore, Py-DDA-Py.

The fluorescence responses of Py-EOA-Py and Py-DDA-Py to the four representative metal ions including Fe^{3+}, Cu^{2+}, Zn^{2+}, and Co^{2+} ion at different concentration were also measured in 7 mM SDS aqueous solutions and displayed in Fig. S6 and S7 (SI). As seen from Fig. S6, the response of Py-EOA-Py to the four metal ions is similar to that of Py-TOA-Py, which retains the cross-reactive responses to different metal ions but shows lower sensitivities. However, as displayed in Fig. S7, Py-DDA-Py exhibits none cross-reactive responses to the tested metal ions. The comparative results of fluorescence variations of Py-TOA-Py, Py-EOA-Py and Py-DDA-Py are illustrated in Fig. 8. Clearly, Py-TOA-Py and Py-EOA-Py exhibit similar response behaviour to the same tested metal ions, whereas Py-DDA-Py shows slight fluorescence variations to these metal ions.

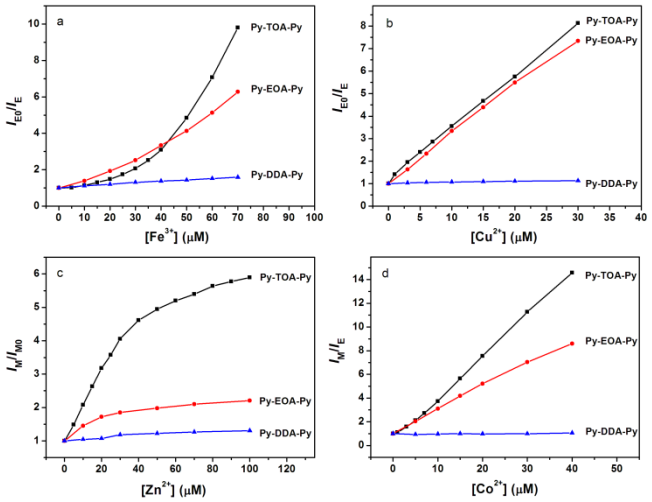

Fig. 8 Fluorescence intensity variation of different fluorophore (1.0 μM) in 7 mM SDS aqueous solution upon addition of different metal ions: (a) Fe^{3+} ion; (b) Cu^{2+} ion; (c) Zn^{2+} ion; (d) Co^{2+} ion.

The similarity possessed by Py-EOA-Py and the remarkable difference possessed by Py-DDA-Py indicate that the hydrophilic structure of the spacer in Py-TOA-Py plays an important role in the versatile fluorescence responses to metal ions. It is well-known that a micelle contains three characteristic regions: a nonpolar core formed by the hydrocarbon tails of amphiphilic molecules, a compact Stern layer having charged head groups, and a wider Gouy-Chapman layer containing the counter ions.[32, 33] Different molecules possessing different hydrophobicity can be located in different regions of micelles.[34] Considering the difference in the spacer polarity, Py-TOA-Py and Py-EOA-Py are expected to locate in the Stern layer region closer to the aggregate-water interface than to the hydrophobic centre due to the hydrophilicity of the spacer in these two compounds. Thus, the environment surrounding fluorophores is loosely packed, then, the two pyrene moieties of Py-TOA-Py and Py-EOA-Py could move flexibly. The addition of metal ions leads to distinct variations of SDS aggregations which further influence the molecular conformation of these fluorophores in the aggregates. By contrast, Py-DDA-Py possessing a hydrophobic spacer is likely to locate in the hydrocarbon core of SDS aggregates and experiences a more compact and restricted microenvironment. Thus, the two pyrene moieties in Py-DDA-Py molecules cannot move freely. The variation of the SDS aggregates induced by metal ions hardly influences the hydrophobic core and leads to less fluorescence changes of Py-DDA-Py.

To verify the above assumptions, time-resolved fluorescence measurements were conducted to provide useful information on excimer formation mechanism, which will help to understand local environments surrounding fluorophores. The time-resolved emission spectra (TRES) of the three bispyrene fluorophores in SDS solutions were measured and the results are displayed in Fig. 9. Apparently, in the early time gate (0-1 ns), the spectrum profiles for Py-TOA-Py and Py-EOA-Py are totally monomer emission. With the time-gate moving to longer times, the contribution from the excimer emission increases and becomes dominative at the time gate longer than 20 ns. These results demonstrate that the excimer of Py-TOA-Py and Py-EOA-Py forms typically via Birks' scheme, where an excited

monomer diffusively encounter with a ground-state molecule and form an excimer, and then return to ground-state.[35, 36] However, for the nonpolar fluorophore, Py-DDA-Py, the excimer emission dominates the whole time gate even as early as 0-1 ns. This result indicates the excimer of Py-DDA-Py is mainly from ground-state dimers, which is called preformed scheme.[35, 36] The difference of excimer formation scheme for fluorophores with different spacers could be related to their locations in the surfactant aggregates. As discussed earlier, Py-TOA-Py and Py-EOA-Py tend to locate at the Stern layer, and Py-DDA-Py prefers to stay in the hydrophobic core of SDS aggregates. Thus, the loosely packed environment of Stern layer enables the two pyrene moieties of Py-TOA-Py and Py-EOA-Py to move smoothly and form dynamic excimer; on the other hand, the densely packed hydrophobic core confines the two pyrene moieties of Py-DDA-Py into restricted environments and makes them form preformed excimer.

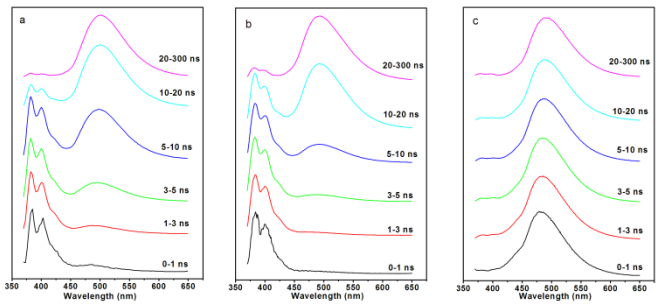

Fig. 9 Time-resolved emission spectra of (a) Py-TOA-Py (1.0 μM), (b) Py-EOA-Py (1.0 μM), and (c) Py-DDA-Py (1.0 μM) in SDS micellar systems (7 mM).

The correlation of excimer formation mechanism with the microenvironment is further verified by examining the excimer formation scheme of Py-TOA-Py in both good and poor solvents. As displayed in Fig. S8 in the SI, in the good solvent, acetonitrile, the excimer formation is time-dependent and follows Birks' scheme. This similarity in excimer formation mechanism of Py-TOA-Py in good solvent to Py-TOA-Py and Py-EOA-Py in SDS solutions confirms that these fluorophores indeed locate at the loosely packed Stern layers and can move freely and flexibly. Oppositely, when tested in the poor solvent, the excimer formation of Py-TOA-Py is time-independent and resembles what observed for Py-DDA-Py in SDS aggregates. It can be imagined that Py-TOA-Py is hard to move freely in the poor solvent since the fluorophore aggressively aggregated in water. The similarity in excimer formation for Py-TOA-Py in water to that for Py-DDA-Py in SDS aggregates only suggests that Py-DDA-Py is located in a restricted microenvironment which should be the hydrophobic core.

Based on the above results and discussion, we could infer that the hydrophilic spacer of Py-TOA-Py draws it to locate closely to the surfactant aggregate-water interface. This location provides a loosely packed microenvironment for the fluorophore and enables the two pyrene moieties to move flexibly. Thus, the photophysical properties of the fluorophore could be easily influenced by the added metal ions (Scheme 3). On one hand, the added metal ions are capable of changing the CMC and aggregation number of micelles, leading to distinct variations of SDS aggregations.[14, 37] As a result, the microenvironment surrounding the fluorescent probe is changed, which gives rise to variation of the geometry of the two pyrene moieties in the bispyrene fluorophore in SDS aggregates. This may answer why there are ratiometric responses to metal ions such as Zn^{2+} and Co^{2+}. On the other hand, some of the tested metal ions are paramagnetic and produce fluorescence quenching to fluorophores via electron transfer, such as Cu^{2+}, Co^{2+}, and Fe^{3+}.[26] Moreover, different metal ions have different ionic radius, electronegativity, polarization force, electron density and so on that lead to the combined force to micelle is various.[38] Then, it further affects the accessibility of metal ions to the surfactant aggregate surface, which may account for the difference in sensitivity. Although it is hard to explain the relationship between particular metal ions and the specific response mode at the current stage, the present work still provides some novelty in developing a single fluorescent sensor system with capability of identifying multiple metal ions and helps to understand the sensing behaviour to some level. As far as the present work is concerned, it shows us that the spacer polarity plays an important role in determining the location of the fluorophore in the surfactant aggregates, and that the location of fluorophore in the supramolecular assemblies influences its sensing behaviour to metal ions.

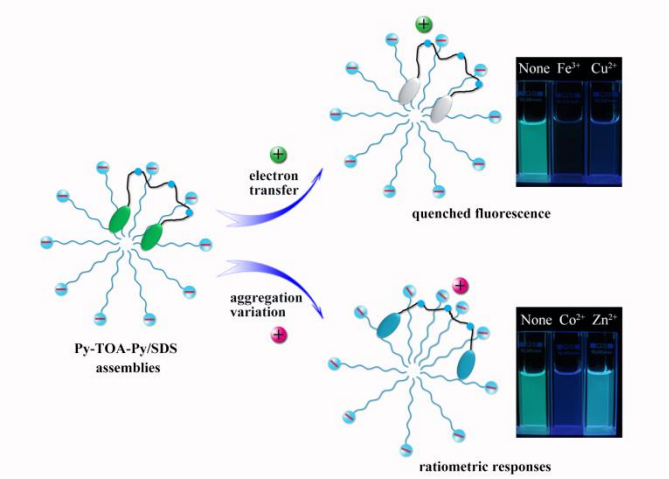

Scheme 3. Schematic cartoon for Py-TOA-Py/SDS sensing different metal ions.

Fluorescence responses to mixed metal ions

The responses of the present sensor system to mixed metal ions were further studied. Firstly, we measured its fluorescence responses to mixtures containing two competing metal ions (Fig. S9 in the SI). Interestingly, we found that the enhanced monomer emission by Zn^{2+} or Co^{2+} still occurs even in the presence of equivalent amount of quencher metal ions such as Fe^{3+} or Cu^{2+} (Fig. S9a - S9d). On the other hand, the excimer quenching by Fe^{3+} and Cu^{2+} is still effective in the presence of equivalent amount of Zn^{2+}. When the two quencher metal ions (Fe^{3+} and Cu^{2+}) co-exist, the sensor system displays quenched monomer and excimer (Fig. S9e). When the two ratiometric metal ions (Zn^{2+} and Co^{2+}) co-exist, a much more significant enhanced monomer is observed along with remarkably decreased excimer emission (Fig. S9f), indicating that excimer decreasing effect of Co^{2+} is also positive in the presence of Zn^{2+}. Secondly, we examined the fluorescence responses to mixtures containing three metal ions (Fig. S10 in the SI). We found that the co-presence of both quencher metal ions (Fe^{3+} and Cu^{2+}) hinders the monomer enhancement effect by either Zn^{2+} or Co^{2+}. At the same time, the monomer quenching effect by Fe^{3+} and Cu^{2+} is also hindered by the presence of either Zn^{2+} or Co^{2+}. We also measured the fluorescence response of the sensor system to the mixtures containing four metal ions (Fe^{3+}, Cu^{2+}, Zn^{2+}, and

Co^{2+}). As seen in Fig. S11 (SI), the co-existence of equivalent amount of the four metal ions results in a ratiometric response of the sensor system. However, a real mixed system is much more complex than the above-examined samples. Therefore, more detailed and systematic studies of mixed systems and a powerful mathematic tool for analysing complex data are needed to evaluate the possibility of the present sensor system to analyse complicated samples, which will be conducted in the near future in our lab.

Conclusions

We have successfully developed a fluorescent supramolecular sensor system, Py-TOA-Py/SDS, capable of pattern recognition of multiple metal ions in aqueous solutions. The sensor system exhibits cross-reactive responses to the 10 tested metal ions. As far as we know, this is the first report that a single sensor system can function as both turn-off and ratiometric sensor at the same time. The combination of fluorescence variation of the bispyrene fluorophore at four selected wavelengths could generate distinct recognition pattern to different metal ions. Moreover, PCA analysis reveals the sensor system could at least discriminate six metal ions including Fe^{3+}, Co^{2+}, Ni^{2+}, Cu^{2+}, Pb^{2+}, and Hg^{2+}.

Synthetic analogue Py-EOA-Py shows similar cross-reactive sensing behaviour to the tested metal ions. However, the control molecule, Py-DDA-Py, with hydrophobic spacer displays none cross-reactive responses to the tested metal ions. Time-resolved emission spectra of the three bispyrene fluorophores in SDS aggregates and that of Py-TOA-Py in both good and poor solvents identify that Py-TOA-Py and Py-EOA-Py locate at hydrophilic water-aggregate interfaces and Py-DDA-Py locates at hydrophobic core. This work reveals that using commercial available surfactants can realize the recognition detection of multiple metal ions by a single organic fluorophore, provided that it contains a hydrophilic spacer which facilitates it to locate near the surfactant aggregate-water interface and to be easily modulated by extra stimuli. Moreover, the present work provides a novel strategy of fabricating discriminative sensors for identifying different metal ions.

Acknowledgements

The authors acknowledge the financial supports from National Natural Science Foundation of China (21173142, 20927001, 21206089), Ministry of Education of China (NCET-12-0895), Shaanxi Provincial Department of Science and Technology (2011KJXX48, 2013JQ2023), the Program of Introducing Talents of Discipline to Universities (B14041), and the Fundamental Research Funds for the Central Universities (GK201301006).

Notes and references

1 A. P. d. Silva, H. Q. N. Gunaratne, T. Gunnlaugsson, A. J. M. Huxley, C. P. McCoy, J. T. Rademacher and T. E. Rice, *Chem. Rev.*, 1997, **97**, 1515-1566.
2 R. Martínez-Máñez and F. Sancenón, *Chem. Rev.*, 2003, **103**, 4419-4476.
3 J. P. Anzenbacher, P. Lubal, P. Bucek, M. A. Palacios and M. E. Kozelkova, *Chem. Soc. Rev.*, 2010, **39**, 3954-3979.
4 S. Rochat, J. Gao, X. Qian, F. Zaubitzer and K. Severin, *Chem. Eur. J.*, 2010, **16**, 104-113.
5 G. V. Zyryanov, M. A. Palacios and P. Anzenbacher Jr., *Angew. Chem. Inter. Ed.* 2007, **46**, 7849-7852.
6 Z. Wang, M. A. Palacios and P. Anzenbacher Jr., *Anal. Chem.* 2008, **80**, 7451-7459.
7 D. C. González, E. N. Savariar and S. Thayumanavan, *J. Am. Chem. Soc.* 2009, **131**, 7708-7716.
8 G. Verma and P. A. Hassan, *Phys. Chem. Chem. Phys.* 2013, **15**, 17016-17028.
9 M. Ramanathan, L. K. Shrestha, T. Mori, Q. Ji, J. P. Hill and K. Ariga, *Phys. Chem. Chem. Phys.* 2013, **15**, 10580-10611.
10 P. Pallavicini, Y. A. Diaz-Fernandez and L. Pasotti, *Coord. Chem. Rev.* 2009, **253**, 2226-2240.
11 P. Bandyopadhyay and A. K. Ghosh, *Sens. Lett.* 2011, **9**, 1249-1264.
12 M. Jamkratoke, G. Tumcharern, T. Tuntulani and B. Tomapatanaget, *J. Fluoresc.* 2011, **21**, 1179-1187.
13 K. Ngamdee, T. Noipa, S. Martwiset, T. Tuntulani and W. Ngeontae, *Sens. Actuators, B* 2011, **160**, 129-138.
14 A. Mallick, M. C. Mandal, B. Haldar, A. Chakrabarty, P. Das and N. Chattopadhyay, *J. Am. Chem. Soc.* 2006, **128**, 3126-3127.
15 S. S. Bag, R. Kundu and S. Talukdar, *Tetrahedron Lett.* 2012, **53**, 5875-5879.
16 J. Wang, X. Qian, J. Qian and Y. Xu, *Chem. Eur. J.* 2007, **13**, 7543-7552.
17 H. Tian, J. Qian, H. Bai, Q. Sun, L. Zhang and W. Zhang, *Anal. Chim. Acta* 2013, **768**, 136-142.
18 R. Hu, J. Feng, D. Hu, S. Wang, S. Li, Y. Li and G. Yang, *Angew. Chem. Inter. Ed.* 2010, **49**, 4915-4918.
19 M. Jamkratoke, V. Ruangpornvisuti, G. Tumcharern, T. Tuntulani and B. Tomapatanaget, *J. Org. Chem.* 2009, **74**, 3919-3922.
20 A. D. Hughes, I. C. Glenn, A. D. Patrick, A. Ellington and E. V. Anslyn, *Chem. Eur. J.* 2008, **14**, 1822-1827.
21 E. N. Savariar, S. Ghosh, D. C. González and S. Thayumanavan, *J. Am. Chem. Soc.* 2008, **130**, 5416-5417.
22 M. A. Palacios, Z. Wang, V. A. Montes, G. V. Zyryanov and P. Anzenbacher, *J. Am. Chem. Soc.* 2008, **130**, 10307-10314.
23 M. Shellaiah, Y.-H. Wu, A. Singh, M. V. R. Raju and H.-C. Lin, *J. Mater. Chem. A*, 2013, **1**, 1310-1318.
24 H. N. Kim, W. X. Ren, J. S. Kim and J. Yoon, *Chem. Soc. Rev.*, 2012, **41**, 3210-3244.
25 S. A. Ezzell and C. L. McCormick, *Water-Soluble Polymers, ACS Symposium Series*, Washington, DC, 1991.
26 L. Ding, S. Wang, Y. Liu, J. Cao and Y. Fang, *J. Mater. Chem. A* 2013, **1**, 8866-8875.
27 L. Ding, Y. Liu, Y. Cao, L. Wang, Y. Xin and Y. Fang, *J. Mater. Chem.*, 2012, **22**, 11574-11582.
28 S. C. McCleskey, M. J. Griffin, S. E. Schneider, J. T. McDevitt and E. V. Anslyn, *J. Am. Chem. Soc.* 2003, **125**, 1114-1115.
29 H. S. Hewage and E. V. Anslyn, *J. Am. Chem. Soc.* 2009, **131**, 13099-13106.
30 H. Li, S.-J. Zhang, C.-L. Gong, Y.-F. Li, Y. Liang, Z.-G. Qi and S. Chen, *Analyst*, 2013, **138**, 7090-7093.
31 T. L. Nelson, C. O'Sullivan, N. T. Greene, M. S. Maynor and J. J. Lavigne, *J. Am. Chem. Soc.* 2006, **128**, 5640-5641.
32 P. Banerjee, S. Pramanik, A. Sarkar and S. C. Bhattacharya, *J. Phys. Chem. B* 2008, **112**, 7211-7219.
33 K. K. Karukstis, S. W. Suljak, P. J. Waller, J. A. Whiles and E. H. Z. Thompson, *J. Phys. Chem.* 1996, **100**, 11125-11132.
34 H. Yan, P. Cui, C.-B. Liu and S.-L. Yuan, *Langmuir* 2012, **28**, 4931-4938.
35 F. M. Winnik, *Chem. Rev.* 1993, **93**, 587-614.
36 L. Ding, Y. Bai, Y. Cao, G. Ren, G. J. Blanchard and Y. Fang, *Langmuir* 2014, **30**, 7645-7653.
37 J.-H. Kim, M. M. Domach and R. D. Tilton, *J. Phys. Chem. B* 1999, **103**, 10582-10590.
38 J. T. McCloskey, M. C. Newman and S. B. Clark, *Environ. Toxicol. Chem.* 1996, **15**, 1730-1737.

Key Laboratory of Applied Surface and Colloid Chemistry of Ministry of Education, School of Chemistry and Chemical Engineering, Shaanxi

Normal University, Xi'an 710062, P. R. China. Fax: 86-29-81530727; Tel: 86-29-81530789; E-mail: dinglp33@snnu.edu.cn

† Electronic Supplementary Information (ESI) available: Chemicals and instruments, synthesis of Py-EOA-Py and Py-DDA-Py, fluorescence stability of Py-TOA-Py in different environments, SDS concentration effect on sensing, fluorescence responses of Py-TOA-Py in SDS solution to Hg^{2+}, Mg^{2+}, Ca^{2+}, Cd^{2+}, Ni^{2+} and Pb^{2+}, fluorescence responses of Py-EOA-Py and Py-DDA-Py in SDS solutions to metal ions, and time-resolved emission of Py-TOA-Py in acetonitrile and water, fluorescence responses to mixed samples. See DOI: 10.1039/b000000x/